

Preprint typeset in JHEP style. - PAPER VERSION

DESY 98-196
MC/TH 98-18
Dec '98
revised Apr '99

Diffractive Photoproduction of Υ at HERA.

L. L. Frankfurt

*Nuclear Physics Department,
School of Physics and Astronomy,
Tel Aviv University, 69978 Tel Aviv, Israel*
E-mail: frankfur@lev.tau.ac.il

M. F. McDermott

*Dept. Physics and Astronomy,
University of Manchester,
Manchester, M13 9PL, England*
E-mail: mm@a13.ph.man.ac.uk

M. Strikman*

*Dept. of Physics, Penn. State University,
University Park, USA*
E-mail: strikman@theow01.desy.de

ABSTRACT: Predictions for the diffractive photoproduction of the Υ -family at HERA energies, within the framework of the analysis by Frankfurt, Koepf and Strikman, are presented. Two novel effects lead to a significant enhancement of the original calculation: the non-diagonal (or skewed) kinematics, calculated to leading-log(Q^2) accuracy, and the large magnitude of the real part of the amplitude. The resultant cross sections are found to agree fairly well with recent preliminary data from ZEUS and H1. A strong correlation between the mass of the diffractively produced state and the energy dependence of the cross section is found. In particular, a considerably stronger rise in energy is predicted than that found in J/ψ -production.

KEYWORDS: Diffraction, Heavy Quarkonium, Non-diagonal distribution.

*current address: Theory Group, DESY, Notkestr. 85, 22607, Hamburg, Germany

hep-ph/9812316 v3 8 Apr 1999



1. Introduction

Diffractive heavy vector meson production was initially evaluated to leading-log accuracy in energy [1], while in [2] all vector mesons were treated to the leading-log accuracy in $\ln Q^2$ and $\ln 1/x$. It is now well understood in QCD, to leading twist accuracy thanks to a generalization of the QCD factorization theorem to hard exclusive processes [3]. So far, for heavy quarkonium production, this knowledge has only been used to confront photo- and electroproduction of J/ψ [4–6]. Unfortunately, the light mass of the charm quark leads to many theoretical uncertainties in the final result (relativistic effects in the wavefunction, scale uncertainties, unitarity corrections...). By studying Υ -production, which has recently been observed in photoproduction for the first time at HERA [7], within the same framework, one may hope to pin down some of these uncertainties.

The current paper is an extension of the work presented by Frankfurt et al [5]. One of the main findings was that the use of realistic light-cone wavefunctions for the heavy vector mesons, $\psi_V(z, k_t)$, with significant average k_t , leads to an overall suppression of the cross-section relative to the static, $\psi_V(z, k_t) = \delta(z - 1/2) \delta^{(2)}(k_t)$, and Gaussian, $\psi_V(z, k_t) = A \delta(z - 1/2) \exp(-ak_t^2/m_c^2)$, forms used in [6]. The hybrid wavefunctions used were designed to interpolate hard QCD behaviour at small transverse distances (normalised to the decay width into leptons) with quarkonium models at large transverse distances. In the limit $m_q^2 \rightarrow \infty$ (but $m_q^2 \ll W^2$) such Fermi-motion effects of the quarks can be substantiated in QCD, because non-quark degrees of freedom will be suppressed by the powers of m_q^2 . Whether such an approximation is applicable to the production of states in the ψ -family is an open question. The k_t -suppression was tempered by an enhancement due to a rescaling (beyond leading-log(Q^2)) of the gluon density to higher scales, to reflect more accurately the typical transverse size of the scattering dipoles.

Here, we present predictions for diffractive (also called exclusive) photoproduction of the Υ -family using similar hybrid wavefunctions. One of our main results is that the non-diagonal (hereafter *skewed*) kinematics lead to a significant enhancement of the cross section. We present an estimate of the size of this effect, to the leading-log accuracy with which the skewed splitting functions are known. At HERA energies $\Upsilon(ns)$ -states are produced at large effective scales (around 40, 60 and 75 GeV² for $n = 1, 2, 3$, respectively) and at relatively high- x (between 0.001 and 0.02). It follows that the real part of the amplitude is large and we calculate it using a fit to the energy dependence of the imaginary part and dispersion relations. Taking both effects into account leads to cross-sections which concur with the measured ones and rise very steeply with W^2 , the γP centre-of-mass energy (approximately $W^{2(0.85)}$).

This note is organised as follows. Firstly, we very briefly recap the relevant equations in [5]. Secondly, we discuss the rescaling procedure in detail. We then explain how the skewedness is calculated and implemented. Next, we give an explanation of the calculation of the real part of the amplitude. Finally, we present and discuss the

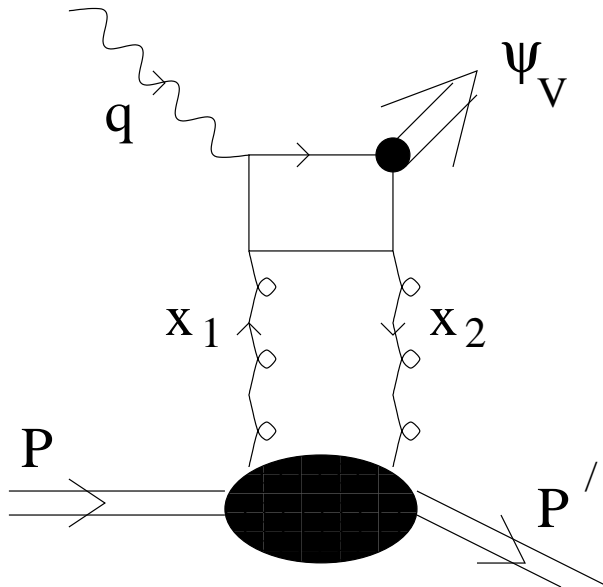


Figure 1: Photoproduction of Heavy Vector mesons

resultant cross-sections, and conclude.

2. Formulae for cross sections

Hard exclusive processes factorize in QCD [3] and at small- x are driven by the exchange of two gluons in the t -channel. One such process is the diffractive electroproduction of heavy vector mesons, in which the exchanged gluons are connected to the $q\bar{q}$ -pair fluctuation of the photon (virtuality $q^2 = -Q^2$) in the four possible ways (one of which is shown in fig.(1)) and convoluted with $\psi_V(z, k_t)$. The forward differential cross-section for a vector meson, mass M_V , containing a (current) quark of mass m , can be written as the product of an asymptotic expression and a finite Q^2 correction, $\mathcal{C}(Q^2)$ (see [5] for more details) :

$$\frac{d\sigma_{\gamma^{(*)}P \rightarrow VP}}{dt} \Big|_{t=0} = \frac{12\pi^3 \Gamma_V M_V^3}{\alpha_{em} (Q^2 + 4m^2)^4} \times$$

$$|\alpha_s(Q_{eff}^2) (1 + i\beta) x G_N(x, Q_{eff}^2)|^2 \left(1 + \epsilon \frac{Q^2}{M_V^2}\right) \mathcal{C}(Q^2), \quad (2.1)$$

with

$$\mathcal{C}(Q^2) = \left(\frac{\eta_V}{3}\right)^2 \left(\frac{Q^2 + 4m^2}{Q^2 + 4m_{run}^2}\right)^4 T(Q^2) \frac{R(Q^2) + \epsilon \frac{Q^2}{M_V^2}}{1 + \epsilon \frac{Q^2}{M_V^2}}, \quad (2.2)$$

where $Q_{eff}^2(Q^2)$, Γ_V , ϵ are the effective transverse scale, the leptonic decay width and photon's polarisation respectively; β is the ratio of real to imaginary parts of the amplitude. The k_t -suppression factor T , R and η_V contain integrals involving the light-cone wavefunctions of the photon and vector meson. Hybrid wavefunctions are used which are designed to have the characteristic $z(1-z)$ behaviour at very small transverse distances expected from QCD (this implies $\eta_V = 3$). This justifies the use of the QCD running mass and hence the correction for this in eq.(2.2). Overall the use of the hybrid wavefunctions, in place of the pure non-relativistic wavefunctions, does not lead to significant effects in the cross sections. In this paper we use the particular model of the quarkonium wavefunction due to Buchmueller and Tye [8]. They used a QCD-inspired potential, with a Coulomb piece corresponding to t-channel gluon exchange ($\propto 1/r$) and a confinement piece ($\propto r$). The analysis produced a value of $m_b = 4.88$ GeV for the quark mass. The significant QCD radiative corrections to the amplitude of heavy quarkonium transition into $q\bar{q}$ -pair are accounted for by normalising the short-distance part of the hybrid light-cone wavefunctions to the width of heavy quarkonium decay into leptons. The analysis of [5] indicated that once the short-distance corrections were included (for transverse distances less than $b_0 = 0.1$ GeV $^{-1}$) several potential models produced similar results. As a result, we expect that the resultant model uncertainty is less than that from other sources and only consider the potential of [8].

In the photoproduction limit we have

$$\sigma(\gamma P \rightarrow VP) = \frac{3\pi^3 \Gamma_V M_V^3 (1 + \beta^2)}{64 \alpha_{EM} (m^2)^4 B_{D,V}} \left[\alpha_s(Q_{eff}^2) xg(x, Q_{eff}^2) \right]^2 \mathcal{C}(Q^2 = 0), \quad (2.3)$$

where, as usual, an exponential decay in $|t|$ is assumed, with $B_{D,V}$ the slope parameter. Since these parameters have not yet been measured, we are forced to estimate them. The established trend is that the slope parameter decreases with increasing vector meson mass. This is a geometrical effect: most of B_D comes from the proton end of the ladder where the typical transverse momenta are much smaller, the upper end contributes progressively less as the typical transverse momentum scales involved increase. On this basis we expect $B_{D,\Upsilon}$ to be a little less than that measured in photoproduction of J/ψ : $B_{D,J/\psi} = 4.4 \pm 0.3$ GeV $^{-2}$ (H1). For the purpose of this paper we assume, for each state, the same value as that measured in electroproduction of J/ψ by H1, $B_{D,V} = 3.9$ GeV $^{-2}$ (see [9] and references therein), since the typical transverse scales at the upper vertices in these processes are similar. Of course, this introduces a further overall uncertainty in the normalisation of the cross sections of about 10 – 20%.

3. Rescaling: calculation of Q_{eff}^2

The procedure that we use for determining the scale, Q_{eff}^2 , in eq.(2.3) is similar to that described in sec.(IIIa) of [4]. The amplitude for the photoproduction of Υ in co-ordinate

space is given by:

$$A(\gamma_T P \rightarrow V_T P) \propto \int_0^1 \frac{dz}{z(1-z)} \int_0^\infty d^2 b_t m_{run}^2 \psi_{\gamma,T}(z, b_t) \hat{\sigma}(b_t^2) \psi_{V,T}(z, b_t), \quad (3.1)$$

where,

$$\hat{\sigma}(b_t^2) = \frac{\pi^2}{3} b_t^2 \alpha_s(b_t^2) xg(x, b_t^2) \quad (3.2)$$

is the cross section for scattering a $q\bar{q}$ dipole of transverse size b_t^2 off the proton (b_t is the conjugate variable to k_t). This quantity is expected to be universal. $\psi_{\gamma,T}(z, b_t) = K_0(b m_{run})$ and $\psi_{V,T}(z, b_t)$ are the light-cone wavefunctions of the transversely-polarised real photon and heavy vector meson in configuration space, respectively.

In order to proceed we need to establish the relation between transverse sizes and momentum scales, such as Q_{eff}^2 , to determine the scale at which we must sample the gluon density and α_s in eq.(3.2). We establish this relation using the expression for the longitudinal structure function written in b_t -space:

$$\sigma_L(x, Q^2) \propto \int dz \int_0^\infty d^2 b_t \hat{\sigma}(b_t^2) |\psi_{\gamma,L}(z, b_t)|^2. \quad (3.3)$$

We now assume that for a particular fixed x, Q^2 the product of transverse size and the momentum scale squared is constant, $b_t^2 Q^2 = \lambda$, with b_t^2 measured in $\text{GeV}^{-2} = b_t^2 (\text{fm}^2)/(\text{hc})^2$, with $\text{hc} = 0.197 \text{ GeV fm}$. We establish this constant from the typical or average transverse sizes contributing to the b_t -integral above. The average b_t^2 is defined to be that value up to which we must integrate in order to reach half of the full b_t^2 integral in eq.(3.3). This average value is fed back into the integral via $\lambda = \langle b_t^2 \rangle Q^2$. The integral is recalculated, sampling the gluon and α_s at $\lambda / \langle b_t^2 \rangle$ and a new median b_t^2 is found. The procedure is then iterated to convergence. It turns out that the resultant λ depends weakly on x, Q^2 . Table.(1) shows λ for a wide range of these kinematic variables (in [5] a constant value of $\lambda = 8.5$ at $x = 10^{-3}$ is used for J/ψ).

Now we have established the relation between transverse size and momentum scales we can use it to set the scale of $\hat{\sigma}(b_t^2)$ in the b_t -integral in eq.(3.1). This allows us to establish the effective scale for the production of each state, by a procedure similar to that used above. With some starting assumption for Q_{eff}^2 we use $\lambda(x, Q_{eff}^2)/b_t^2$ as the scale at which xg, α_s, m_{run}^2 are sampled in the integral. This requires some regulation at very small and very large values of b_t^2 , however, the contributions to the overall integral from these regions are negligible. We establish the median $b^2 = \langle b^2 \rangle$ for this integral, as above. This is then fed back in via $Q_{eff}^2(\text{new}) = \lambda(x, Q_{eff}^2(\text{old})) / \langle b^2 \rangle$ and the procedure is iterated to convergence.

In this way the value of the effective scale depends on the dominant values of b_t^2 . Dipoles in the photon which most closely correspond to the relevant s-wave state, (have the ‘‘right transverse size’’ and momentum sharing z) contribute most to the production. The rescaling procedure is designed to reflect this. The scale varies depending on

x	Q^2	10	30	50	70	90
1.0×10^{-3}		8.51	10.8	11.5	11.8	12.0
		8.80	10.7	11.1	11.4	11.7
5.0×10^{-3}		9.82	12.3	12.9	13.2	13.4
		10.2	12.1	12.5	12.7	12.9
9.0×10^{-3}		10.4	12.8	13.5	13.8	13.9
		10.8	12.7	13.0	13.5	13.6
1.3×10^{-2}		10.8	13.3	13.9	14.1	14.3
		11.1	13.0	13.4	13.7	13.8
1.7×10^{-2}		11.2	13.7	14.3	14.6	14.7
		11.3	13.3	13.7	13.8	14.0

Table 1: $\lambda(x, Q^2)$ as a function of x and Q^2 (GeV²). The upper values refer to CTEQ4L partons and the lower to MRSTLO.

	x	0.001	0.005	0.009	0.013	0.017
Υ	CTEQ	37	40	40	40	41
	MRST	41	42	42	42	43
Υ'	CTEQ	58	61	62	63	65
	MRST	57	60	62	63	65
Υ''	CTEQ	71	76	77	80	80
	MRST	70	75	76	78	79

Table 2: The effective scale, Q_{eff}^2 in GeV², for each s-wave Υ -state as a function of x

the state in question since the relevant light-cone wavefunctions weight the integral in eq.(3.1) differently. The resulting effective scale, Q_{eff}^2 , depends weakly on x and strongly on the state concerned (see table.(2)).

The fact that Q_{eff}^2 increases with the mass of the state agrees with [4, 5] and is perhaps counter-intuitive given that the quarks are less tightly bound in the higher s-wave states, leading to larger typical sizes. It is worth remembering, however, that the precise momentum scale is governed by a convolution of the photon and vector meson light-cone wavefunctions, and that higher states also contain nodes which further confuses the issue from an intuitive point of view. In fact, the typical transverse momenta contributing to the production of these higher mass states is larger (see table.(3)) and this is reflected in the larger Q_{eff}^2 . The precise values of this effective scale are sensitive to the details of the vector meson wavefunction. The outlined rescaling procedure represents a reasonable estimate given the current knowledge of this quantity.

4. Calculation of the effect of skewedness

Recently, there has been considerable progress in calculating and understanding skewed parton distributions, which probe new non-perturbative information about hadrons and are a generalisation of conventional parton distributions (for an extensive list of references see [10]). The former replace the latter in expressions for hard exclusive cross-sections. They are relevant for a wide range of hard exclusive processes such as deeply-virtual Compton scattering, diffractive dijets in photoproduction, and most importantly for our purposes, photo- and electroproduction of vector mesons.

In the latter processes, the skewedness, δ , arises from the need to convert a space-like $q^2 = -Q^2$, into a time-like M_V^2 , and is given by the difference in momentum fractions carried by the outgoing (x_1) and returning (x_2) gluons (see fig.(1)),

$$x_1 = \frac{M_{q\bar{q}}^2 + Q^2}{W^2 + Q^2}, \quad x_2 = \frac{M_{q\bar{q}}^2 - M_V^2}{W^2 + Q^2}, \quad (4.1)$$

$$\delta = x_1 - x_2 = \frac{M_V^2 + Q^2}{W^2 + Q^2}, \quad (4.2)$$

where $M_{q\bar{q}}^2$ is the mass of the intermediate $q\bar{q}$ -state. In terms of the light-cone variables it is given by

$$M_{q\bar{q}}^2 = \frac{k_t^2 + m_q^2}{z(1-z)}. \quad (4.3)$$

For photoproduction of Υ at HERA, $\delta = M_\Upsilon^2/W^2$ is small and lies in the range $\{0.0011, 0.017\}$, although it is an order of magnitude larger than for J/ψ -photoproduction in the same energy range.

It was argued in [11] that for small x and for Q_0^2 , where parton densities weakly depend on x , the dependence on δ can be neglected. It was further demonstrated in [11] that for large Q^2 and small x the main contribution to the skewed parton densities comes from the parton densities at Q_0^2 scale where $\tilde{x} \gg x$, for which the skewedness is very small. Hence the answer for these kinematics does not depend on this approximation. Freund and Guzey [12] have modified the DGLAP-evolution [13] package of the CTEQ collaboration [14], which is based on a numerical grid integration, to produce the skewed gluon functions, $G_\delta(x_1, Q^2)$, for any x_1 at a fixed value of δ (it is straightforward to write an interpolating subroutine to obtain G for any δ). We use this code and the approximation that the skewed and conventional distributions are the same at the starting scale, Q_0^2 .

It is then sufficient to replace the conventional splitting functions with their skewed generalisations in the evolution (i.e. $P_{ab}(x) \rightarrow P_{ab}(\delta, x)$). Unfortunately the latter are only known to leading-log accuracy at present (although, very recently progress has been reported [15] on the next-to-leading order). For consistency one is forced

to use only leading-log parton distributions at the input scale; we use the two most recent leading-order distributions, i.e. CTEQ4L [16] and MRSTLO¹ [17], and evolve to leading-log(Q^2) accuracy. The code produces the skewed gluon distribution $G_\delta(x_1, Q_{eff}^2)$ to replace the ordinary gluon density, $xg(x, Q_{eff}^2)$ of eq.(2.3). The two distributions are shown in fig.(2), in the relevant x -range for $Q_{eff}^2 = 40 \text{ GeV}^2$ characteristic of $\Upsilon(1s)$ -production (see table.(2)). This replacement leads to an overall enhancement factor of about $(1.6)^2 \simeq 2.6$ for $\Upsilon(1s, 2s, 3s)$ cross-sections.

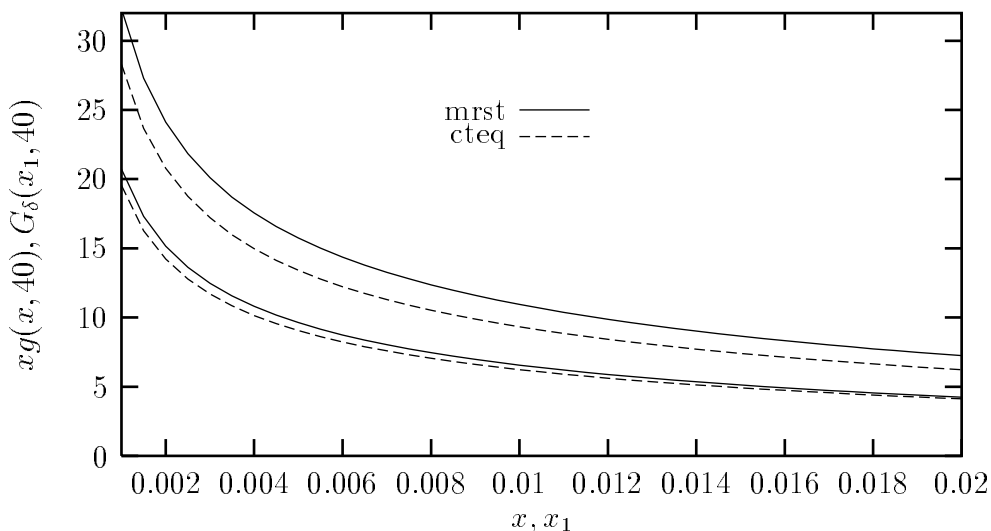


Figure 2: A comparison of skewed and conventional gluon densities at a scale of $Q^2 = 40 \text{ GeV}^2$, the effective scale for Υ -photoproduction. Conventional leading-order input distributions are used in both cases (at starting scales $Q_0^2 = 1.6$ and 1.0 GeV^2 for CTEQ4L [16] and MRSTLO [17], respectively). The skewed distributions are the upper curves and have fixed $x_1/\delta = 1.2$.

It is necessary to determine the appropriate value of x_1 to use. We estimate this by calculating the average values of transverse momentum and light-cone momentum sharing $\langle k_t \rangle$ and $\langle z \rangle$ contributing to $M_{q\bar{q}}^2$ in the relevant loop integral. A more accurate calculation would integrate explicitly over $M_{q\bar{q}}^2$, but in this case all direct connection to the measured forward distribution, and hence predictability, would be lost (until the input densities for skewed evolution have been explicitly measured themselves).

The amplitude of eq.(3.1) is used to calculate the relevant value of $M_{q\bar{q}}^2$ for the particular value of W . First of all we calculate $\langle z \rangle$. We then integrate over z , take a Fourier transform back to k_t -space and calculate the median value of the k_t -integral by the method outlined above for calculating medians of integrals. Both $\langle z \rangle$ and $\langle k_t^2 \rangle$ are then fed into eq.(4.3) to determine $M_{q\bar{q}}^2$. The range of values of $\langle k_t^2 \rangle$ and typical $\langle z \rangle$ for each s-wave state are shown in table.(3). The result depends weakly on energy, W . Table.(4) shows the resultant values of $x_1/\delta = M_{q\bar{q}}^2/M_V^2$ as a function of

¹We thank R. Roberts for providing the parameters at the starting scale.

W for the three s-wave states. The code for calculating the cross sections automatically takes this variation into account.

Note that as soon as x_1/δ is small we are not sensitive to a specific value of this ratio since in this limit the ratio of skewed and diagonal densities weakly depends on x_1/δ . This justifies the use of the conventional distributions in $\hat{\sigma}$ when calculating $M_{q\bar{q}}^2$.

		$\langle k_t^2 \rangle$ (80 GeV)	$\langle k_t^2 \rangle$ (280 GeV)	$\langle z \rangle$
Υ	CTEQ	4.04	5.34	0.40
	MRST	4.54	5.90	0.40
Υ'	CTEQ	4.88	6.20	0.28
	MRST	5.43	6.71	0.28
Υ''	CTEQ	5.90	7.34	0.26
	MRST	6.50	7.78	0.26

Table 3: Averages of k_t^2 and z for each s-wave Υ -state.

	W (GeV)	80	130	180	230	280
Υ	CTEQ	1.14	1.16	1.17	1.18	1.19
	MRST	1.17	1.20	1.21	1.22	1.24
Υ'	CTEQ	1.23	1.26	1.28	1.29	1.30
	MRST	1.28	1.30	1.32	1.33	1.34
Υ''	CTEQ	1.28	1.30	1.32	1.33	1.34
	MRST	1.32	1.35	1.36	1.37	1.38

Table 4: The ratio x_1/δ for each s-wave Υ -state as a function of W .

5. Calculating the real part of the amplitude

It is convenient to use the dispersion representation in energy to calculate the real part of the scattering amplitude. In doing so we automatically take into account a possible contribution of the region of $x_1 > 0, x_2 < 0$ in the real part. Previously, the ratio of real to imaginary parts of the amplitude, β , was calculated using the approximate solution of this dispersion relation:

$$\beta = \frac{\pi}{2} \frac{d \ln(xg(x, Q^2))}{d \ln(1/x)}, \quad (5.1)$$

first derived in [18], and used in [4–6]. This is appropriate at small x and fairly low scales where the gluon density and hence the imaginary part of the amplitude may be approximated by a single power in energy ($ImA \propto xg/x \propto (W^2)^\alpha$). The result is then $\beta = \frac{\pi}{2}(\alpha - 1)$, for α sufficiently close to 1.

W (GeV)	Υ		Υ'		Υ''		Υ (eq.(5.1))
	CTEQ	MRST	CTEQ	MRST	CTEQ	MRST	CTEQ
80	1.25	1.27	1.55	1.56	1.78	1.78	0.88
130	0.76	0.79	0.89	0.91	0.94	0.99	0.68
180	0.62	0.65	0.71	0.73	0.72	0.78	0.60
230	0.55	0.58	0.63	0.64	0.63	0.68	0.56
280	0.51	0.54	0.58	0.59	0.58	0.63	0.53

Table 5: Relative contribution of the real part of the amplitude, β^2 , as a function of W for photoproduction of $\Upsilon(1s)$, $\Upsilon(2s)$, $\Upsilon(3s)$. For comparison the last column shows the values of β^2 obtained for Υ using eq.(5.1), sampling the CTEQ4L gluon at $Q_{eff}^2 = 40\text{GeV}^2$.

At the larger values of x and higher scales, Q_{eff}^2 , relevant to photoproduction of Υ -states it is necessary to include an additional sub-leading power in $1/x$ or equivalently in W^2 . For fixed x_1/δ (we use the values at $W = 180$ GeV, see table.(4)) and Q_{eff}^2 the skewed gluon distribution is a function of W^2 only. We perform a two-power Regge-type fit to this distribution, at the relevant fixed effective scale, over the whole range in W^2 using MINUIT [19]:

$$G_\delta(x_1, Q_{eff}^2) = aW^{2b} + cW^{2d}. \quad (5.2)$$

We may then use analyticity of the amplitude directly to construct a dispersion relation and hence determine β ,

$$\beta(W) = \frac{ReA}{ImA} = -\frac{aW^{2(b+1)} \cot\left(\frac{\pi(b+1)}{2}\right) + cW^{2(d+1)} \cot\left(\frac{\pi(d+1)}{2}\right)}{aW^{2(b+1)} + cW^{2(d+1)}}. \quad (5.3)$$

Table.(5) shows how β^2 changes as a function of W , these values are used in the cross sections of eq.(2.3). For a comparison, we also show the values of β^2 for Υ using eq.(5.1). As expected these differ most for smaller values of W .

6. Results

The cross section for photoproduction of the Υ states is

$$\sigma(\gamma P \rightarrow VP) = \frac{3\pi^3 \Gamma_V M_V^3 (1 + \beta^2)}{64 \alpha_{em} (m^2)^4 B_{D,V}} \left[\alpha_s(Q_{eff}^2) g_\delta(x_1, Q_{eff}^2) \right]^2 \mathcal{C}(Q^2 = 0). \quad (6.1)$$

The effective scale, Q_{eff}^2 , x_1/δ and β^2 all depend on the state concerned and weakly on energy as indicated in the tables.(2,4,5) above. The overall suppression factor, $\mathcal{C}(Q^2 = 0)$ is given by

$$\mathcal{C}(Q^2 = 0) = \left(\frac{m^2}{m_{run}^2} \right)^4 \left[\frac{m_{run}^6 \int \frac{dz}{z(1-z)} \int db b^3 \psi_{V,T}(z, b) \psi_\gamma(z, b)}{M_V^2 \int \frac{dz}{z(1-z)} \psi_{V,T}(z, b=0)} \right]^2. \quad (6.2)$$

The resolution of the muon chambers at the HERA experiments is such that the three contributing s-wave states $\Upsilon, \Upsilon', \Upsilon''$ are not resolved [7]. Hence, what is actually measured is the sum of the production rates of the mesons times their respective branching fractions to muons ($\text{Br}(\Upsilon(n\text{s}) \rightarrow \mu^+\mu^-) = 2.48, 1.31, 1.81\%$ for $n = 1, 2, 3$, respectively [21]). In fig.(3) we present our predictions for this measured quantity using MRST (upper solid curve) and CTEQ (lower solid curve) input parton distributions. This illustrates the agreement of the model with the data collected so far. Also shown (dashed curves) are the predictions for $\Upsilon(1\text{s})$ alone for the two input distributions. There are two reasons why the MRST curves should be higher than CTEQ curves. Firstly, the skewed parton distributions are higher (see Fig.(2)). Secondly, smaller values for Λ_{QCD} are used in MRSTLO than in CTEQ4L, this makes the value of α_s larger at a given effective scale.

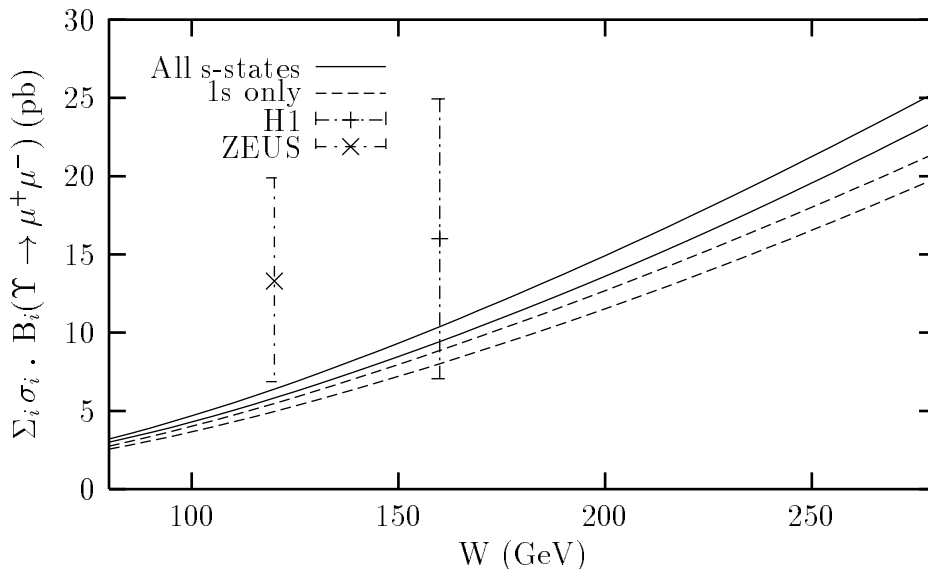


Figure 3: Sum of cross sections times branching ratios to muons for $\Upsilon(1\text{s}), \Upsilon'(2\text{s}), \Upsilon''(3\text{s})$ as a function of energy. The dashed curves are for $\Upsilon(1\text{s})$ alone. The upper (lower) curves in each case correspond to MRSTLO (CTEQ4L) partons at the starting scale. Also shown are the data from ZEUS and H1 (preliminary), at their respective mean energies, with systematic and statistical errors added in quadrature.

Fig.(4) shows our prediction for the photoproduction of $\Upsilon(1\text{s})$ as function of energy in the HERA range, using both input distributions. A very steep rise is expected, as can be seen from the figure, this corresponds approximately to $W^{1.7}$ over the range shown, i.e. almost a full power in W stronger than that seen in J/ψ production (a recent fit [9] to ZEUS and H1 data revealed a power of 0.8 ± 0.1). This very steep rise is due to the sampling of the gluon at the large scale, $Q_{eff}^2 \simeq 40 \text{ GeV}^2$, where it is rising steeply with energy. In practice the steepness of the observed rise may prove to be a useful way to discriminate between models which have rescaling and those that do not, since for a fixed range in x the steepness increases with scale.

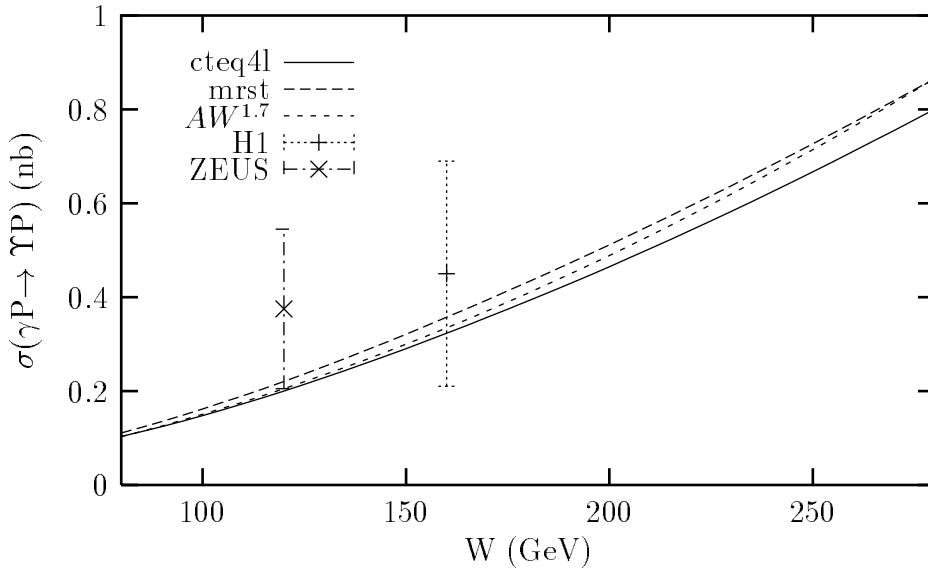


Figure 4: Cross section for photoproduction of $\Upsilon(1s)$ in the HERA energy range, compared to values quoted by the HERA experiments [7] at their respective mean energies. An additional curve, $AW^{1.7}$, with A normalised to the CTEQ4L cross section at $W = 80$ GeV, is also shown to indicate the very steep rise with energy.

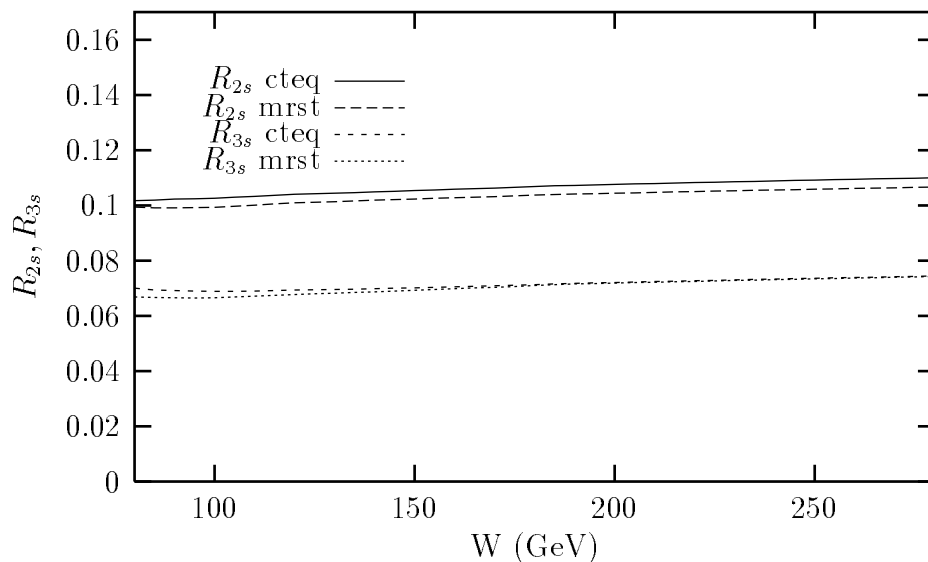


Figure 5: Ratios of cross-sections times branching ratio to muons: $R_{2s} = \sigma B(2s)/\sigma B(1s)$, $R_{3s} = \sigma B(3s)/\sigma B(1s)$.

Figure.(5) shows predictions for ratios of the products of cross-sections and branching ratios to muons, for the Υ' , Υ'' relative to Υ as a function of energy. The different k_t -suppression factors for the different states (for CTEQ4L $C(Q^2 = 0) = 0.290, 0.139, 0.0820$, for MRSTLO $C(Q^2 = 0) = 0.283, 0.138, 0.0817$, respectively) imply that the relative rates of the three states are not expected to be the same as those found at CDF [20],

and used by ZEUS and H1 to unfold and produce a cross section for $\Upsilon(1s)$ production. The CDF data implies that $\Upsilon(1s)$ is responsible for about 70% of the signal whereas our calculation indicates a larger value of about 85% (see also fig.(3)). For this reason a comparison of the predictions in Fig.(4) with the values quoted by the experiments (also shown), must be done with care.

Although the states cannot be separated this predominance of $\Upsilon(1s)$ should reflect itself in the average observed value of the mean mass of the muon pair in the signal.

7. Conclusions and discussion

We have presented predictions for the cross sections of diffractive photoproduction of Υ -states in the HERA range, based on a previous analysis [5]. In this paper two new effects, the off-diagonal nature of the amplitude and the largeness of its real part are found to be important and lead to a significant enhancement of the normalisation of the cross sections. We perform a reanalysis of rescaling procedure used to set the scale of the production of the three s-wave states. We find good agreement with the first data from HERA. One striking prediction of the analysis is a very strong rise of the cross sections with energy which is driven by the skewed gluon density (see eq.(6.1) and fig.(2))

Throughout the paper we have used the hybrid light-cone wavefunctions suggested in [5], which were constructed to agree with quarkonium wavefunctions at large distances and QCD at small distances. These wavefunctions have significant Fermi motion of the quarks inside the bound states. Gauge invariance demands that if one has finite- k_t one also needs gluonic degrees of freedom. So far only the contribution to the cross section of the lowest order Fock states of the vector meson and photon ($|b\bar{b}\rangle$) have been considered. The next step is to calculate higher order Fock states which also include the gluon degrees of freedom. The connection between these light-cone wavefunctions and quarkonium wavefunctions derived from solving the Schrödinger equation for a particular potential remains an open question, which such a calculation would begin to address.

Acknowledgments

The authors gratefully acknowledge Werner Köpf, Andreas Freund and Vadim Guzey for providing and explaining various computer codes. We also thank the referee for his valuable suggestions. M.M. is happy to acknowledge PPARC for financial assistance (grant number: GR/L56244). M.S. would like to thank DESY for hospitality during the time this work was done. The work of M.S and L.F. is supported by the U.S. Department of Energy and BSF.

References

- [1] M. G. Ryskin *Z. Physik C* **57** (1993) 89.
- [2] S. J. Brodsky et al, *Phys. Rev. D* **50** (1994) 3134.
- [3] J. C. Collins *Phys. Rev. D* **57** (1998) 3051;
J. C. Collins, L. L. Frankfurt, M. Strikman, *Phys. Rev. D* **56** (1997) 2982.
- [4] L. L. Frankfurt, W. Köpf, M. Strikman, *Phys. Rev. D* **54** (1996) 3194.
- [5] L. L. Frankfurt, W. Köpf, M. Strikman, *Phys. Rev. D* **57** (1998) 512.
- [6] M. G. Ryskin et al, *Z. Physik C* **76** (1997) 231.
- [7] ZEUS collab., hep-ex/9807020, DESY-98-089;
H1 collab., “Observation of Υ -Production at HERA”,
paper 574, ICHEP98, Vancouver, available from
<http://www-h1.desy.de/h1/www/publications/conf/list.vancouver98.html>
- [8] W. Buchmüller and S.-H. H. Tye., *Phys. Rev. D* **24** (1981) 132.
- [9] H1 collab., “Diffractive Charmonium production in DIS at HERA”,
paper 572, ICHEP98, Vancouver, available from
<http://www-h1.desy.de/h1/www/publications/conf/list.vancouver98.html>
- [10] X.-D. Ji, *J. Phys. G* **24** (1998) 1181 .
- [11] L.L. Frankfurt et al, *Phys. Lett. B* **418** (1998) 345, Erratum-ibid. *Phys. Lett. B* **429** (1998) 414.
- [12] A. Freund and V Guzey, hep-ph/9801388; hep-ph/9806267.
- [13] V.N. Gribov and L.N. Lipatov, *Sov. J. Nucl. Phys.* **15** (1972) 438;
G. Altarelli and G. Parisi, *Nucl. Phys. B* **126** (1977) 298;
Yu.L. Dokshitzer, *Sov. Phys. JETP* **46** (1977) 641.
- [14] CTEQ collab., see CTEQ meta page on
<http://www.phys.psu.edu/~cteq/> for details.
- [15] A.V. Belitsky et al, hep-ph/9810275.
- [16] H. Lai et al, *Phys. Rev. D* **55** (1997) 1280.
- [17] A. Martin et al, hep-ph/9808371.
- [18] V. N. Gribov and A. A. Migdal, *Sov. J. Nucl. Phys.* **8** (1969) 583.
- [19] F. James, “MINUIT: function minimization and Error analysis”,
CERN Program Library Long Writeup D506.
- [20] CDF Collab., F. Abe et al, *Phys. Rev. Lett.* **75** (1995) 4358.
- [21] Particle Data Group. *Euro. Phys. J.* **3** (1998) 1-4.